# Spatial Sigma-Delta Massive MIMO: Improved Channel Estimation and Achievable Rates

Shilpa Rao[1], Hessam Pirzadeh[1], Gonzalo Seco-Granados[2], and A. Lee Swindlehurst[1]

[1]Center for Pervasive Communications and Computing, University of California, Irvine
[2]Department of Telecommunications and Systems Engineering, Universitat Autonoma de Barcelona

*Abstract*—**Spatial $\Sigma\Delta$ sampling has recently been proposed to improve the performance of massive MIMO systems with low-resolution quantization for cases where the users are confined to a certain angular sector, or the array is spatially oversampled. We derive a linear minimum mean squared error (LMMSE) channel estimator for the $\Sigma\Delta$ array based on an element-wise Bussgang decomposition that reformulates the nonlinear quantizer operation using an equivalent linear model plus quantization noise. Both the case of one- and two-bit quantization is considered. We then evaluate the achievable rate of the $\Sigma\Delta$ system assuming that a linear receiver based on the LMMSE channel estimate is used to decode the data. Our numerical results demonstrate that $\Sigma\Delta$ architecture is able to achieve superior channel estimates and sum spectral efficiency compared to conventional low-resolution quantized massive MIMO systems.**

## I. Introduction

Low-resolution quantization has recently been proposed as a potential method for reducing the energy consumption and hardware complexity of massive MIMO systems for uplink communication [1–6]. While the performance degradation of such systems is small at very low signal-to-noise ratios (SNRs), the loss grows rapidly with SNR. Performance near that achievable without any quantization can be obtained if the resolution is increased to 4-5 bits [7], or if the sampling rate is increased [8], [9], but these adjustments come with significant increases in both complexity and the required data rate from the remote radio head to the baseband processor.

Temporal $\Sigma\Delta$ ADCs combine one-bit quantization with oversampling [10], [11] to create a noise-shaping effect that reduces the impact of the coarse ADC. However, the oversampling again increases the fronthaul throughput compared with standard one-bit quantization. To remedy this issue, recent work has considered a *spatial* version of the $\Sigma\Delta$ concept for massive MIMO [12–16], in which the noise shaping gain is achieved either by oversampling in space (more closely-spaced antennas), or by assuming users whose uplink signals arrive from a given angular sector due to cell sectorization, limited multipath scattering, or certain small-cell geometries.

In this paper, we derive an improved channel estimator for spatial $\Sigma\Delta$ massive MIMO systems compared to our initial approach described in [14], which was based on a vector version of the Bussgang decomposition previously used in channel estimation for standard one-bit quantization [1]. Instead, in this work we use an element-wise Bussgang approach that defines the quantization noise in a way that is more consistent with the spatial $\Sigma\Delta$ architecture [16]. The Bussgang decomposition provides an equivalent linear signal-plus-quantization-noise model that we exploit to derive a linear minimum mean-squared error (LMMSE) channel estimator. We derive the solution for both the cases of one- and two-bit quantization. Using an approach similar to [1], [3], [17], we then find a lower bound on the uplink rate achieved by a linear receiver calculated using our LMMSE channel estimate. A more detailed analysis of the bounds on the achievable rate and the estimation error are presented in [18]. The simulation results for channel estimation and spectral efficiency for maximal ratio combining (MRC) and zero-forcing (ZF) receivers are promising and show that the $\Sigma\Delta$ architecture significantly outperforms standard 1-2 bit quantization.

This work was supported by the U.S. National Science Foundation under Grants CCF-1703635 and ECCS-1824565.

## II. System Model

We assume an uplink scenario in which an $M$-antenna base station (BS) simultaneously receives signals from $K$ single-antenna users. Assuming the users synchronously transmit $N$-sample pilot sequences, the received signal, $\mathbf{X} \in \mathbb{C}^{M\times N}$, at the BS is

$$\mathbf{X} = \sqrt{\rho}\,\mathbf{G}\,\mathbf{\Phi}_t + \mathbf{N}, \tag{1}$$

where $\mathbf{G} \in \mathbb{C}^{M\times K}$ is the channel matrix, $\mathbf{\Phi}_t \in \mathbb{C}^{K\times N}$ is the pilot matrix and $\mathbf{N}$ is additive zero-mean spatially-white Gaussian noise $\mathbf{N} \sim \mathcal{CN}(\mathbf{0}, \mathbf{I})$. We assume that the pilot sequences are orthogonal and that the minimum number of pilots are used, so that $N = K$ and $\mathbf{\Phi}_t\mathbf{\Phi}_t^H = K\mathbf{I}_K$. We will further assume that power control is applied so that all the user signals are received with the same power. Therefore, the SNR is equal to $\rho$. Note that since $\mathbf{\Phi}$ is unitary, the power of the pilot symbols is time-invariant: $\mathbf{\Phi}_t^H\mathbf{\Phi}_t = K\mathbf{I}_K$.

We will assume that the uplink signal from each user arrives via $L$ coherent paths that lie within a certain contiguous angular sector defined by $\Theta$. The BS is equipped with a uniform linear array (ULA), so the $k$th column of $\mathbf{G}$, $\mathbf{g}_k$, representing the channel for the $k$th user, is given by

$$\mathbf{g}_k = \frac{1}{\sqrt{L}}\mathbf{A}\mathbf{h}_k, \tag{2}$$

where the elements of $\mathbf{h}_k$ are i.i.d. as $\mathcal{CN}(0,1)$ random variables, and $\mathbf{A} \in \mathbb{C}^{M\times L}$ is a matrix whose $l$th column is the steering vector

$$\mathbf{a}_l = \left[1 \;\; e^{-j2\pi\delta\sin(\theta_l)} \;\; \dots \;\; e^{-j2\pi\delta(M-1)\sin(\theta_l)}\right]^T, \tag{3}$$

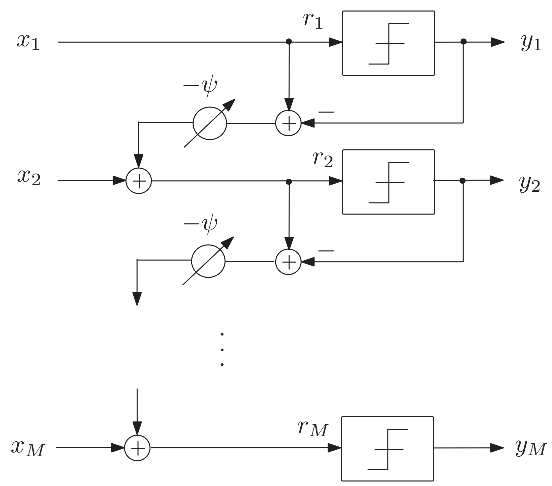


Fig. 1: A first-order one-bit $\Sigma\Delta$ array steered to direction $\psi$.

where $\delta = d/\lambda$ is the inter-element antenna spacing and $\theta_l, l = 1, \ldots, L$, lie in the sector $\left[-\frac{\Theta}{2}, \frac{\Theta}{2}\right]$. Thus, the channel $\mathbf{G}$ is given by $\mathbf{G} = \frac{1}{\sqrt{L}}\mathbf{A}\mathbf{H}$, where $\mathbf{H}$ is matrix whose $k$th column is given by $\mathbf{h}_k$. The above channel model is reflective of a rich scattering environment where the columns of $\mathbf{A}$ are chosen from a dense sampling of steering vectors from the angular sector $\left[-\frac{\Theta}{2}, \frac{\Theta}{2}\right]$. The channel covariance matrix is given by $\mathbf{C}_G = \frac{1}{L}\mathbf{A}\mathbf{A}^H$, which we assume to be known, where $(\cdot)^H$ denotes the conjugate transpose.

Let $\mathbf{\Phi} = \sqrt{\rho}\left(\mathbf{\Phi}_t^T \otimes \mathbf{I}_M\right)$, $\mathbf{g} = \mathrm{vec}\left(\mathbf{G}\right)$ and $\mathbf{n} = \mathrm{vec}\left(\mathbf{N}\right)$, where $\otimes$ represents the Kronecker product. Vectorizing (1) creates the $MN \times 1$ data vector

$$\mathbf{x} = \mathrm{vec}\left(\mathbf{X}\right) = \mathbf{\Phi}\mathbf{g} + \mathbf{n}. \tag{4}$$

It is easy to see that the covariance matrix of $\mathbf{x}$ is

$$\mathbf{C}_x = K\rho\,\mathbf{C}_g + \mathbf{I}_{MN}, \tag{5}$$

where $\mathbf{C}_g = \mathbf{I}_K \otimes \mathbf{C}_G$ is block-diagonal.

## III. Channel Estimation with a First-Order Spatial $\Sigma\Delta$ Architecture

Fig. 1 shows the architecture of a first-order spatial $\Sigma\Delta$ array. The quantization error from one antenna is phase-shifted by $-\psi$ prior to being added to the input of the adjacent antenna, which shifts the error to spatial frequencies away from the angle-of-arrival (AoA) associated with the angle $\psi$. Hence, users in the angular sector around this AoA experience a high signal-to-quantization-noise ratio (SQNR). The high-SQNR angular sector can be extended by increasing the spatial oversampling, or placing the antenna elements closer together. In practice, however, mutual coupling limits the amount of spatial oversampling that can be achieved.

We will define $\mathbf{r}$ as the $MN \times 1$ vector of inputs to the quantizers, and $\mathbf{y}$ as the $MN \times 1$ vector output of the $\Sigma\Delta$-array. Because of the vectorization in (4), the $m$th element $\{x_m, r_m, y_m\}$ of each vector $\{\mathbf{x}, \mathbf{r}, \mathbf{y}\}$ corresponds to antenna $\mathrm{mod}_M(m)$, where $\mathrm{mod}_M(\cdot)$ denotes the modulo-$M$ operator. Defining $m' = \mathrm{mod}_M(m)$, we thus have

$$y_m = \alpha_{m'}\mathcal{Q}_{m'}\left(\mathrm{Re}(r_m)\right) + j\alpha_{m'}\mathcal{Q}_{m'}\left(\mathrm{Im}(r_m)\right), \tag{6}$$

where $\mathcal{Q}_{m'}$ represents the quantization operator and $\alpha_{m'}$ is an output gain, both of which may vary with $m'$. We will see later that with an appropriate input automatic gain control, the dependence on $m'$ can be eliminated. Thus, the output of the $\Sigma\Delta$ array can be written as

$$\begin{aligned} \mathbf{y} &= \mathcal{Q}(\mathbf{r}) \\ &= \left[\mathcal{Q}_1(r_1), \ldots, \mathcal{Q}_M(r_M), \mathcal{Q}_1(r_{M+1}), \ldots, \mathcal{Q}_M(r_{MN})\right]^T, \end{aligned} \tag{7}$$

where

$$\begin{aligned} \mathbf{r} &= \mathbf{U}\mathbf{x} - \mathbf{V}\mathbf{y}, \\ \mathbf{V} &= \mathbf{I}_N \otimes \underbrace{\begin{bmatrix} 0 & 0 & \ldots & 0 & 0 \\ e^{-j\psi} & 0 & \ldots & 0 & 0 \\ e^{-j2\psi} & e^{-j\psi} & \ldots & 0 & 0 \\ & & \vdots & & \\ e^{-j(M-1)\psi} & e^{-j(M-2)\psi} & \ldots & e^{-j\psi} & 0 \end{bmatrix}}_{\mathbf{V}_d}, \\ \mathbf{U} &= \mathbf{I}_N \otimes \underbrace{\left(\mathbf{I}_M + \mathbf{V}_d\right)}_{\mathbf{U}_d}. \end{aligned} \tag{8}$$

### A. Equivalent Linear Model

We will describe the operation of the $\Sigma\Delta$ array using an equivalent linear model given by

$$\mathbf{y} = \mathbf{\Gamma}\mathbf{r} + \mathbf{q}\,, \tag{9}$$

where the quantization "noise" term $\mathbf{q}$ is simply defined to be the difference between the actual output and that predicted by the linear model defined by the matrix $\mathbf{\Gamma}$. Different choices of $\mathbf{\Gamma}$ will lead to different quantization noise models with different statistical properties. In our initial work on channel estimation for the $\Sigma\Delta$ array [14], we followed the approach used in [1] for conventional one-bit quantization and obtained the matrix $\mathbf{\Gamma}$ as the one that forces $\mathbf{r}$ to be uncorrelated with $\mathbf{q}$, i.e. $\mathbb{E}\left[\mathbf{r}\mathbf{q}^H\right] = 0$. This results in $\mathbf{\Gamma} = \mathbf{C}_{yr}\mathbf{C}_r^{-1}$, where $\mathbf{C}_{yr} = \mathbb{E}\left[\mathbf{y}\mathbf{r}^H\right]$ and $\mathbf{C}_r = \mathbb{E}\left[\mathbf{r}\mathbf{r}^H\right]$. We then assumed the elements of $\mathbf{r}$ to be jointly Gaussian, and applied the Bussgang theorem to obtain the LMMSE channel estimate. However, this approach produces an equivalent quantization noise $\mathbf{q}$ that does not have a physical interpretation in terms of the hardware block diagram of Fig. 1, since for example the quantizer input $r_m$ at antenna $m$ is clearly correlated with the quantization noise $q_{m-1}$ from the adjacent antenna.

Instead, here we will apply the Bussgang decomposition one element of $\mathbf{y}$ at a time, and define $\mathbf{\Gamma}$ in order to obtain an equivalent linear model for which the elements of $\mathbf{y}$ and $\mathbf{r}$ are only individually uncorrelated [16]: $\mathbb{E}\left[r_m\bar{q}_m\right] = 0$, where $\bar{(\cdot)}$ indicates conjugation. Assuming as before that the elements of $\mathbf{r}$ are circularly symmetric Gaussian random variables, $\mathbf{\Gamma}$

becomes a diagonal matrix with $m$th diagonal element, $\gamma_m$, given by

$$\gamma_m = \frac{\mathbb{E}\left[\operatorname{Re}\left(r_m\right)\operatorname{Re}\left(y_m\right)\right]}{\mathbb{E}\left[\operatorname{Re}\left(r_m\right)\right]^2} = \alpha_{m'}\frac{\mathbb{E}\left[\operatorname{Re}\left(r_m\right)\mathcal{Q}_{m'}\left(\operatorname{Re}(r_m)\right)\right]}{\mathbb{E}\left[|\operatorname{Re}\left(r_m\right)|^2\right]}. \tag{10}$$

We will choose $\alpha_{m'}$ such that $\gamma_m = 1$, or equivalently such that $\mathbf{\Gamma} = \mathbf{I}_{MN}$.

Define $\sigma_{r_m}^2 \triangleq \mathbb{E}\left(|r_m|^2\right)$ and similarly for $\sigma_{y_m}^2$ and $\sigma_{q_m}^2$. For a zero-mean unit-variance Gaussian random variable, define the optimal quantization levels and intervals as $\nu_i$ and $\left(\nu_i^{\mathrm{lo}}, \nu_i^{\mathrm{hi}}\right)$, $i = 1, \ldots, 2^b$, respectively, where $b$ is the resolution of the quantizer. We will focus on one and two-bit quantizers, so that $b = 1$ and $b = 2$, respectively. Since we assume the input to the $m$th $\Sigma\Delta$ ADC is a circularly symmetric Gaussian random variable with variance $\sigma_{r_m}^2$, the quantization bins are adjusted as follows to span the range of the input levels:

$$\mathcal{Q}_{m'}\left(r_m^{\mathrm{Re}}\right) = \frac{\sigma_{r_m}}{\sqrt{2}}\nu_i, \quad \text{if } r_m^{\mathrm{Re}} \in \left(\frac{\sigma_{r_m}}{\sqrt{2}}\nu_i^{\mathrm{lo}}, \frac{\sigma_{r_m}}{\sqrt{2}}\nu_i^{\mathrm{hi}}\right], \tag{11}$$

where $r_m^{\mathrm{Re}} \triangleq \operatorname{Re}\left(r_m\right)$ and the quantization thresholds satisfy $\nu_i^{\mathrm{hi}} = \nu_{i+1}^{\mathrm{lo}}$, $\nu_1^{\mathrm{lo}} = -\infty$, and $\nu_{2^b}^{\mathrm{hi}} = \infty$. For one-bit ADCs the levels of the unit quantizer are $\{-1, +1\}$, and for two-bit ADCs, the levels are chosen according to [19]. Using Price's theorem [20], we can obtain

$$\frac{\mathbb{E}\left[r_m^{\mathrm{Re}}\mathcal{Q}_{m'}\left(r_m^{\mathrm{Re}}\right)\right]}{\mathbb{E}\left[|r_m^{\mathrm{Re}}|^2\right]} = \frac{1}{\sqrt{2\pi}}\sum_{i=2}^{2^b}\left(\nu_i - \nu_{i-1}\right)\exp\left(-\frac{\left(\nu_i^{\mathrm{lo}}\right)^2}{2}\right). \tag{12}$$

Details for the derivation of (12) can be found in [18]. The value of $\alpha_{m'}$ that yields $\gamma_m = 1$ is obtained by substituting (12) in (10).

It is clear from the above results that $\alpha_{m'}$ does not depend on the index $m'$ since the quantization levels and intervals for the $m'$th ADC have been scaled by the standard deviation of the input in (11), e.g., by means of an automatic gain control at the input. Thus, we will drop the dependence of $\alpha$ on $m'$ and choose the single value $\alpha_*$ necessary to achieve $\gamma_m = 1$. Note also that the result in (12) relies on the assumption that $r_m$ is Gaussian. In reality, due to the non-linear feedback structure of the $\Sigma\Delta$ array, the tails of the distribution of $r_m$ are slightly heavier than a Gaussian, so the ratio on the left hand side of (12) is slightly greater than the right hand side. For this reason, we will adopt a slightly larger value for $\alpha_*$:

$$\alpha_* = \begin{cases} \beta\sqrt{\frac{\pi}{2}}, & b = 1, \\ \beta\frac{\sqrt{2\pi}}{\sum_{i=2}^{4}(\nu_i - \nu_{i-1})\exp\left(-\frac{\left(\nu_i^{\mathrm{lo}}\right)^2}{2}\right)}, & b = 2. \end{cases}, \tag{13}$$

where $\beta > 1$ is a correction factor. While we could set $\beta = 1$ as in [16], better channel estimation results are obtained when a value slightly larger than one is used. The value of $\beta$ will be discussed below.

Substituting $\mathbf{\Gamma} = \mathbf{I}$ and $\mathbf{r} = \mathbf{U}\mathbf{x} - \mathbf{V}\mathbf{y}$ into (9), we get

$$\mathbf{y} = \mathbf{x} + \mathbf{U}^{-1}\mathbf{q}\,. \tag{14}$$

This model can be interpreted as passing $\mathbf{x}$ through a (spatial) all-pass filter and $\mathbf{q}$ through a filter that shapes the quantization noise away from the AoA corresponding to $\psi$ [16], which is the spatial analog of the standard temporal $\Sigma\Delta$ approach.

### B. LMMSE Channel Estimation

We derive below the LMMSE channel estimate based on the one-bit or two-bit outputs of the $\Sigma\Delta$ ADC array. The LMMSE channel estimate is defined by

$$\begin{aligned}\hat{\mathbf{g}} &= \mathbb{E}\left[\mathbf{g}\mathbf{y}^H\right]\left(\mathbb{E}\left[\mathbf{y}\mathbf{y}^H\right]\right)^{-1}\mathbf{y} \\ &= \mathbf{C}_{gy}\mathbf{C}_y^{-1}\mathbf{y}\,.\end{aligned} \tag{15}$$

Using the analysis from Appendix A of [18], we can show that $\mathbb{E}\left[\mathbf{x}\mathbf{q}^H\right] \approx \mathbf{0}$ and $\mathbb{E}\left[\mathbf{n}\mathbf{q}^H\right] \approx \mathbf{0}$, which implies that $\mathbf{C}_{gy} \approx \mathbf{C}_g\mathbf{\Phi}^H$. In [18], we validate these approximations by showing the agreement between the theoretical and experimental values of the channel estimation error and the achievable user rate. Since we have chosen $\mathbf{\Gamma} = \mathbf{I}$ in (9), it is easy to show that

$$\mathbf{r} = \mathbf{x} - \mathbf{U}^{-1}\mathbf{V}\mathbf{q} \tag{16}$$

and hence that

$$\mathbf{C}_r = \mathbf{C}_x + \mathbf{U}^{-1}\mathbf{V}\mathbf{C}_q\mathbf{V}^H\mathbf{U}^{-H}, \tag{17}$$

where $\mathbf{C}_q$ is the covariance matrix of $\mathbf{q}$. Given the inter-relationship between $\mathbf{C}_y$ and $\mathbf{C}_q$, they cannot be computed in closed form. However, the nature of the signal propagation in the $\Sigma\Delta$ array allows us to compute them in a recursive manner.

Since $\mathbb{E}\left[r_m\bar{q}_m\right] = 0$ and $\mathbb{E}\left[\mathbf{x}\mathbf{q}^H\right] \approx \mathbf{0}$, it is straightforward to show that $\mathbb{E}\left[q_m\bar{q}_{m\pm 1}\right] \approx 0$. Thus, $\mathbf{C}_q$ is approximately diagonal with elements given by $\sigma_{q_m}^2$. Given that $\mathbf{U}^{-1}\mathbf{V}$ has the special structure

$$\mathbf{U}^{-1}\mathbf{V} = \mathbf{I}_N \otimes e^{-j\psi}\begin{bmatrix} 0 & 0 & \ldots & 0 & 0 \\ 1 & 0 & \ldots & 0 & 0 \\ 0 & 1 & \ldots & 0 & 0 \\ & & \vdots & & \\ 0 & 0 & \ldots & 1 & 0 \end{bmatrix}, \tag{18}$$

we can generate the following recursion for $\sigma_{r_m}^2$, $\sigma_{y_m}^2$ and $\sigma_{q_m}^2$, each computed one after the other:

$$\begin{aligned}\sigma_{r_m}^2 &= \begin{cases} \sigma_{x_m}^2, & m = kM + 1, \quad k = 0, 1, \ldots, M-1, \\ \sigma_{x_m}^2 + \sigma_{q_{m-1}}^2, & \text{otherwise.} \end{cases} \\ \sigma_{y_m}^2 &= \begin{cases} \frac{\pi}{2}\beta^2\sigma_{r_m}^2, & b = 1, \\ \alpha_*^2\sigma_{r_m}^2\sum_{i=1}^{4}\nu_i^2\left(\Psi\left(\frac{\sigma_{r_m}}{\sqrt{2}}\nu_i^{\mathrm{hi}}\right) - \Psi\left(\frac{\sigma_{r_m}}{\sqrt{2}}\nu_i^{\mathrm{lo}}\right)\right), \\ \qquad b = 2 \end{cases} \\ \sigma_{q_m}^2 &= \sigma_{y_m}^2 - \sigma_{r_m}^2.\end{aligned} \tag{19}$$

Here, $\Psi\left(\cdot\right)$ is the cumulative distribution function (cdf) of the standard normal distribution. Once the diagonal matrix $\mathbf{C}_q$ is computed, we can obtain $\mathbf{C}_r$ from (17), and using (14) we can obtain the covariance matrix of $\mathbf{y}$ from

$$\mathbf{C}_y = \mathbf{C}_x + \mathbf{U}^{-1}\mathbf{C}_q\mathbf{U}^{-H}. \tag{20}$$

From the last equality in (19), we can see that for the one-bit $\Sigma\Delta$ operation to be stable, the quantization noise power must not become greater than $\sigma^2_{r_m}$. This requires that we ensure $\left(\frac{\pi}{2}\beta^2 - 1\right) < 1$, and hence that $1 \le \beta < 2/\sqrt{\pi} \approx 1.1284$. We have found that good performance for the one-bit $\Sigma\Delta$ quantizer can be achieved using a value near the midpoint, *e.g.,* $\beta \approx 1.05$. For the two-bit $\Sigma\Delta$ case, on the other hand, there is little dependence on $\beta$ since increasing the number of bits results in a quantization error that is more accurately characterized as Gaussian.

## IV. Uplink Achievable Rate Analysis

In the uplink data transmission stage, the $K$ users transmit their data represented by the $K \times 1$ vector $\mathbf{s}$. Using a Bussgang decomposition on the $\Sigma\Delta$-quantized received signal, $\mathbf{y}_d$,

$$\mathbf{y}_d = \mathcal{Q}\left(\mathbf{r}_d\right) = \sqrt{\rho_d}\mathbf{G}\mathbf{s} + \mathbf{n}_d + \mathbf{U}_d^{-1}\mathbf{q}_d, \tag{21}$$

where $\mathbf{r}_d = \mathbf{U}_d\left(\sqrt{\rho_d}\mathbf{G}\mathbf{s} + \mathbf{n}_d\right) - \mathbf{V}_d\mathbf{y}_d$, $\rho_d$ is the data transmission power, $\mathbf{n}_d$ and $\mathbf{q}_d$ are the noise and quantization noise in the data phase, respectively. The matrices $\mathbf{U}_d$ and $\mathbf{V}_d$ are defined by taking $N = 1$ in Eq. (8).

The BS uses a linear receiver $\mathbf{W} = [\mathbf{w}_1 \; \cdots \; \mathbf{w}_K]$ for symbol detection that depends on the LMMSE channel estimate:

$$\hat{\mathbf{s}} = \mathbf{W}^H\mathbf{y}_d = \sqrt{\rho_d}\mathbf{W}^H\mathbf{G}\mathbf{s} + \mathbf{W}^H\mathbf{n}_d + \mathbf{W}^H\mathbf{U}_d^{-1}\mathbf{q}_d. \tag{22}$$

We can re-write the various components contributing to the $k$th detected symbol as

$$\begin{aligned}\hat{s}_k =& \sqrt{\rho_d}\mathbb{E}\left[\mathbf{w}_k^H\mathbf{g}_k\right]s_k + \sqrt{\rho_d}\left(\mathbf{w}_k^H\mathbf{g}_k - \mathbb{E}\left[\mathbf{w}_k^H\mathbf{g}_k\right]\right)s_k + \\ & \sqrt{\rho_d}\mathbf{w}_k^H\sum_{i\neq k}\mathbf{g}_i s_i + \mathbf{w}_k^H\mathbf{n}_d + \mathbf{w}_k^H\mathbf{U}_d^{-1}\mathbf{q}_d,\end{aligned} \tag{23}$$

where the first term in the above equation corresponds to the desired signal. The remaining terms correspond to the receiver uncertainty, the inter-user interference, the additive noise and the quantization noise, respectively. We will use the classical approach of assuming worst-case uncorrelated Gaussian assumption on the terms in (23) to obtain a lower bound on the achievable rate, which is given by (24) at the top of the next page. While the achievable rate bounds derived in [16] assume perfect knowledge of the CSI, our result takes into account the channel estimation error.

## V. Simulation Results

This section provides some numerical examples of the (per-antenna) normalized MSE (NMSE) of the channel estimates and the resulting sum spectran efficiency (SE) achieved by the $\Sigma\Delta$ massive MIMO system with both one and two-bit outputs. In these examples, the BS employs a uniform linear array (ULA) with inter-element spacing $\delta = 1/5$, the number of pilot symbols and number of users are both 12 ($N = K = 12$), and $\rho_d = \rho$. The users are located within a sector centered on the broadside of the array with an angular spread of $\Theta = 50°$, so $\psi = 0°$. The number of coherent paths per user is $L = 50$. The NMSE of the channel estimate is evaluated over 500 independent realizations of the channel. We will evaluate the performance of the MRC and ZF receivers, given by

$$\mathbf{W}_{\mathrm{MRC}} = \hat{\mathbf{G}}, \qquad \mathbf{W}_{\mathrm{ZF}} = \hat{\mathbf{G}}\left(\hat{\mathbf{G}}^H\hat{\mathbf{G}}\right)^{-1}, \tag{25}$$

where $\hat{\mathbf{G}}$ is the LMMSE channel estimate. The sum spectral efficiency is defined as

$$\mathrm{SE} = \frac{T-N}{T}\sum_{i=1}^{K} R_k, \tag{26}$$

where $T = 200$ is length of the coherence interval.

In Fig. 2, we compare the performance of the $\Sigma\Delta$ LMMSE channel estimator derived in this paper with the standard one-bit Bussgang LMMSE (BLMMSE) channel estimator of [1] and the LMMSE channel estimator for standard two-bit quantization (see [18] for details on implementation of this approach). For this case, an array of $M = 200$ antennas is assumed. At low-to-medium SNRs, the performance of the $\Sigma\Delta$ channel estimates is very close to that of the unquantized MMSE channel estimate. At higher SNRs, the NMSE error floor for the $\Sigma\Delta$ approach is approximately 10dB lower than that achieved with standard one-bit or two-bit ADCs. Note that all algorithms are exploiting knowledge of $\mathbf{C}_g$, which incorporates the *a priori* information about the users' angular sector. The method in [14] fails to provide good channel estimates beyond an SNR of 0dB.

In Fig. 3, we plot the simulated sum spectral efficiency (SE) lower bound for the MRC and ZF receivers as a function of the number of antennas, $M$ for an SNR of 0dB. Fig. 3(a) shows that the SE of the $\Sigma\Delta$ architecture with only one or two bits of ADC resolution is essentially equal to that of an unquantized system, although for MRC the gain compared to standard one- and two-bit quantization is not as dramatic since multi-user interference is more of a limiting factor in this case. Much bigger gains are evident for the case of a ZF receiver, as shown in Fig. 3(b). For $M = 200$ antennas, the throughput bound for the spatial $\Sigma\Delta$ architecture is twice that for regular one- and two-bit ADCs.

## VI. Conclusion

In this paper, we used an element-wise Bussgang decomposition to derive a new LMMSE channel estimator for an massive MIMO system employing spatial $\Sigma\Delta$ ADCs with 1-2 bits resolution. The simulation results show that, in situations where the users are confined to a certain angular sector or the array is spatially oversampled, the spatial $\Sigma\Delta$ approach is able to achieve significantly better channel estimates and spectral efficiency than systems employing standard low resolution quantizers. At low-to-medium SNRs, the performance gap between the $\Sigma\Delta$ array and a system with infinite-resolution ADCs is relatively small. The spatial $\Sigma\Delta$ architecture provides a promising approach for increasing the energy efficiency and reducing the hardware complexity and fronthaul throughput requirements of large-scale antenna systems.

$$R_k = \log_2\left(1 + \frac{\rho_d \left|\mathbb{E}\left[\mathbf{w}_k^H \mathbf{g}_k\right]\right|^2}{\rho_d \mathrm{var}\left(\mathbf{w}_k^H \mathbf{g}_k\right) + \rho_d \sum_{i \neq k} \mathbb{E}\left[\left|\mathbf{w}_k^H \mathbf{g}_i\right|^2\right] + \mathbb{E}\left[\left|\mathbf{w}_k^H \mathbf{n}_d\right|^2\right] + \mathbb{E}\left[\left|\mathbf{w}_k^H \mathbf{U}_d^{-1} \mathbf{q}_d\right|^2\right]}\right) \tag{24}$$

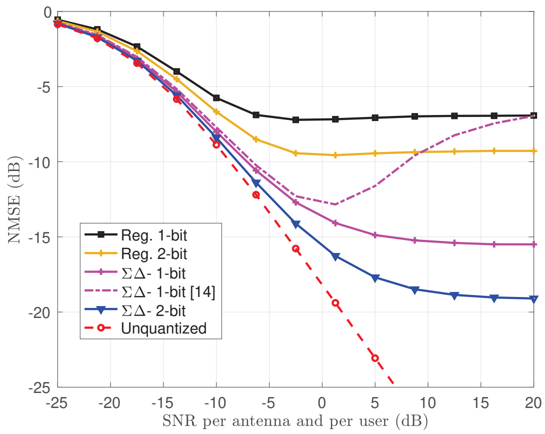


Fig. 2: NMSE of channel estimates.

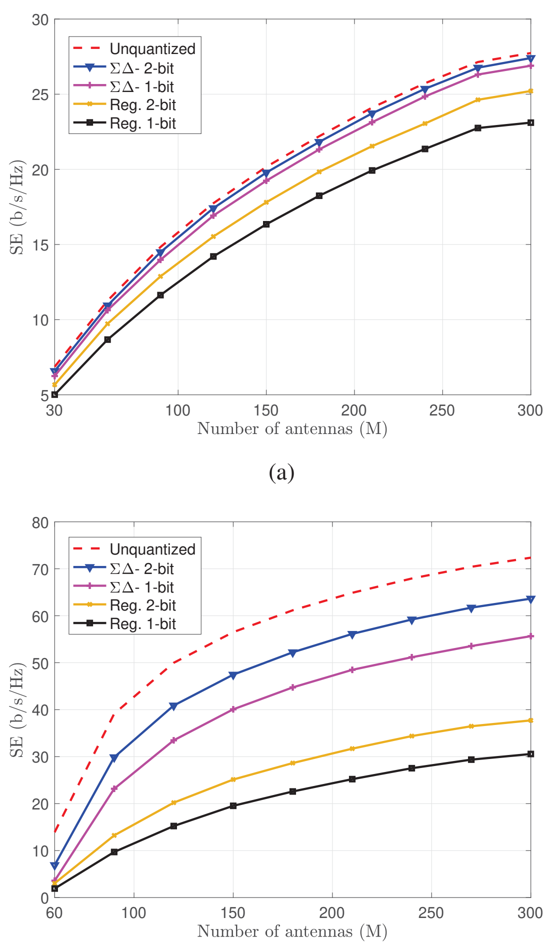


(a)

(b)

Fig. 3: Sum spectral efficiency with (a) MRC (b) ZF receivers.

## REFERENCES


[1] Y. Li, C. Tao, G. Seco-Granados, A. Mezghani, A. L. Swindlehurst, and L. Liu, "Channel estimation and performance analysis of one-bit massive MIMO systems," *IEEE Trans. Signal Process.*, vol. 65, no. 15, pp. 4075–4089, August 2017.

[2] S. Jacobsson, G. Durisi, M. Coldrey, U. Gustavsson, and C. Studer, "Throughput analysis of massive MIMO uplink with low-resolution ADCs," *IEEE Trans. Wireless Commun.*, vol. 16, no. 6, pp. 4038–4051, June 2017.

[3] C. Mollén, J. Choi, E. G. Larsson, and R. W. Heath, "Uplink performance of wideband massive MIMO with one-bit ADCs," *IEEE Trans. Wireless Commun.*, vol. 16, no. 1, pp. 87–100, Jan 2017.

[4] J. Choi, J. Mo, and R. W. Heath, "Near maximum-likelihood detector and channel estimator for uplink multiuser massive MIMO systems with one-bit ADCs," *IEEE Trans. Commun.*, vol. 64, no. 5, pp. 2005–2018, May 2016.

[5] Y.-S. Jeon, N. Lee, S.-N. H., and R. W. Heath, "One-bit sphere decoding for uplink massive MIMO systems with one-bit ADCs," *IEEE Trans. Wireless Commun.*, vol. 17, no. 7, pp. 4509–4521, 2018.

[6] P. Dong, H. Zhang, W. Xu, G. Y. Li, and X. You, "Performance analysis of multiuser massive MIMO with spatially correlated channels using low-precision ADC," *IEEE Commun. Lett.*, vol. 22, no. 1, pp. 205–208, 2017.

[7] K. Roth, H. Pirzadeh, A. L. Swindlehurst, and J. A. Nossek, "A comparison of hybrid beamforming and digital beamforming with low-resolution ADCs for multiple users and imperfect CSI," *IEEE J. Sel. Topics Sig. Proc.*, vol. 12, no. 3, pp. 484–498, June 2018.

[8] A. B. Üçüncü and A. Ö. Yilmaz, "Oversampling in one-bit quantized massive MIMO systems and performance analysis," *IEEE Trans. Wireless Commun.*, 2018.

[9] A. Gokceoglu, E. Björnson, E. G. Larsson, and M. Valkama, "Spatio-temporal waveform design for multiuser massive MIMO downlink with 1-bit receivers," *IEEE J. Sel. Topics Sig. Proc.*, vol. 11, no. 2, pp. 347–362, March 2017.

[10] P. M. Aziz, H. V. Sorensen, and J. Van der Spiegel, "An overview of sigma-delta converters," *IEEE Signal Process. Mag.*, vol. 13, no. 1, pp. 61–84, 1996.

[11] R Gray, "Oversampled sigma-delta modulation," *IEEE Trans. Commun.*, vol. 35, no. 5, pp. 481–489, 1987.

[12] R. M. Corey and A. C. Singer, "Spatial sigma-delta signal acquisition for wideband beamforming arrays," in *Proc. Int. ITG Workshop on Smart Antennas*, March 2016.

[13] D. Barac and E. Lindqvist, "Spatial sigma-delta modulation in a massive MIMO cellular system," M.S. thesis, Department of Computer Science and Engineering, Chalmers University of Technology, 2016.

[14] S. Rao, A. L. Swindlehurst, and H. Pirzadeh, "Massive MIMO channel estimation with 1-bit spatial sigma-delta ADCs," in *Proc. ICASSP*. IEEE, 2019, pp. 4484–4488.

[15] M. Shao, W. Ma, Q. Li, and A. L. Swindlehurst, "One-bit sigma-delta MIMO precoding," *IEEE J. Sel. Topics Sig. Proc.*, vol. 13, no. 5, pp. 1046–1061, Sep. 2019.

[16] H. Pirzadeh, G. Seco-Granados, S. Rao, and A. L. Swindlehurst, "Spectral efficiency of one-bit sigma-delta massive MIMO," *to appear in IEEE J. Sel. Areas Commun. (also available as arXiv preprint arXiv:1910.05491)*, 2019.

[17] Q. Zhang, S. Jin, K.-K. Wong, H. Zhu, and M. Matthaiou, "Power scaling of uplink massive MIMO systems with arbitrary-rank channel means," *IEEE Trans. Signal Process.*, vol. 8, no. 5, pp. 966–981, 2014.

[18] S. Rao, G. Seco-Granados, H. Pirzadeh, and A. L. Swindlehurst, "Massive MIMO channel estimation with low-resolution spatial sigma-delta ADCs," *arXiv preprint arXiv:2005.07752*, 2020.

[19] J. Max, "Quantizing for minimum distortion," *IRE Trans. on Inf. Theory*, vol. 6, no. 1, pp. 7–12, 1960.

[20] R. Price, "A useful theorem for nonlinear devices having Gaussian inputs," *IRE Trans. Inf. Theory*, vol. 4, no. 2, pp. 69–72, 1958.